Study of active beam steering system with a simple method

Jun Wang (王 俊), Lihua Huang (黄立华)*, **Liying Hou (侯莉颖), Guojun He (何国俊),**
Qiang Song (宋 强), and Huijie Huang (黄惠杰)

Shanghai Institute of Optics and Fine Mechanics, Chinese Academy of Sciences, Shanghai 201800, China
*Corresponding author: hlh@siom.ac.cn

We develop a simple method to stabilize the beam during propagation. Combination of the self-developed control module and the large diameter mirrors reconstruct the beam stabilization system, and some important procedures are presented, such as calibration and average filter. The results show that the horizontal pointing and vertical pointing are stabilized to within 8.43 and 7.59 μrad, and the beam horizontal position and vertical position are stabilized to within 2.16 and 2.11 μm respectively. The regulating time is within 84 ms. Thus the method presented is effective for the current stabilization system applied in lithography tools.

OCIS codes: 140.0140, 140.3425.
doi: 10.3788/COL201412.081405.

Variations in laser beam pointing or position can be a serious problem and maintaining a stable beam is a crucial element in many laser-based applications, such as medical treatment[1], industrial processing[2], writing fiber Bragg gratings[3], interferometer measurements[4], inertial confinement fusion[5], high-resolution radiography using laser produced X-rays[6], optical tracking[7], scanning beam interference lithography[8,9], high-power laser[10], optical nonlinear index measurements[11], fiber lasers[12], and so on. Actually, fluctuations of laser beam position and pointing have existed along the large propagation paths from the light source to the target plane due to the thermal expansion and contraction of the optical elements and even vibration of platform. Generally, the beam stabilization is used to correct either the beam pointing deviation or the beam position deviation[13−15]. If the pointing and position deviation are restrained simultaneously, a complicated control algorithm is required due to the coupling between pointing and position[9,16].

For the existing stabilization setup, fast steering mirrors (FSMs) with the small diameter are adopted to direct the beam, and commercial acquisition module for example the National Instruments board to achieve the signal from the sensors. Some systems require a sophisticated procedure on the laser beam and cannot be applied to long distance applications[17]. While nrad stabilization over kilometers of distance has been achieved[18], key components such as the phase modulator and beam recycling cavity cannot be applied to the actual lithography tools. In the earlier work, in order to perform the verifying experiment, our group has also established a beam stabilization system to correct the pointing and position drifts simultaneously by using matrix algorithm[16].

However, in the actual lithography tools, because of the long transmission path (∼20 m), and the large spot size (∼1 inch diameter), and the instability of the pointing and position of ArF laser, the large diameter mirror is required. Besides, for the sake of being integrated with the whole lithography tools, self-developed control system and simple algorithm are essential.

In this work, we adopt a laser diode (LD) as the light source and the large diameter FSMs (ϕ75 mm) provided by Fan group of the National University of Defense Technology (NUDT), and develop a data acquisition and control unit based on the TMS320F2812 chip to reconstruct the beam stabilization system. Also, we propose a simple method for the stabilization system which can reduce the standard deviation for beam position and pointing further and show less regulating time because of more directly controlling than that of the matrix algorithm. As a result, the stabilization performance can satisfy the requirements of the lithography tools, and the key components and the modified method also can be installed into the lithography tools directly.

The reconstructed beam stabilization is presented in Fig. 1, which includes the laser source, the beam steering unit (BSU), the beam measurement unit (BMU), and relay optical element. The laser source goes through few relay optical elements to the FSM-1 and FSM-2 of the BSU and then only 5% beam is directed into the BMU that can measure the beam pointing and position directly[16]. The FSMs have same performances including angular range about +10 mrad and 5 μrad resolution, and 10 μrad repeatability and 250 Hz closed-loop amplitude bandwidth.

The layout of the experiment (Fig. 1) described in this letter is the same as that used in Ref. [19], but it occurs that proposing an optimal stabilization method as a replacement of the matrix algorithm, which is running in our self-developed control module as shown core board
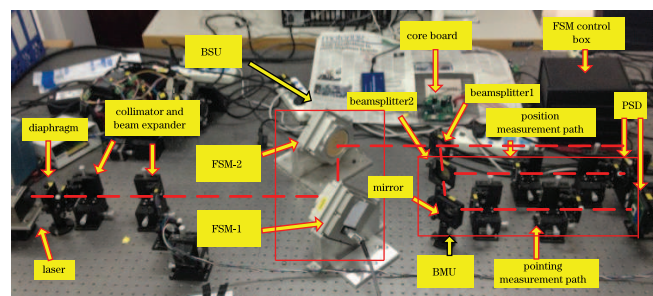

Fig. 1. Test platform for beam stabilization.

in Fig. 1. Besides, compared with the small diameter mirror, the FSMs bearing the larger and heavier mirror have slower response and worse accuracy. In order to overcome these differences, and to improve the performance of the steering system, we make better control methods.

The control system for implementing beam stabilization is illustrated in block diagram in Fig. 2. Position sensitive detectors (PSDs) in the BMU sample the beam pointing drifting and displacement deviation. PSDs processing circuits and A/D conversion circuits digitize the sensor signals and feed them to the controller. Algorithms in the controller process the sensors data and generate commands to move the FSMs. Each FSM has two axes, allowing us to independently control the four beam stabilization errors.

It can be seen that the BMU can achieve the beam pointing and position drifts which is just the right aim for beam stabilization. Therefore, we can take a consideration if the control process gets quicker and easier through achieving the beam drifts directly than that of using matrix algorithm. After the beam drifts measurement and proportion conversion, we can obtain the control command for the BSU.

Figure 3 shows the beam correction fundamental principle. If one defines the mirror rotating angle θ and the distance H between the mirrors in Fig. 3, the beam pointing change $\Delta\theta$ and position displacement Δx can be given by

$$\Delta\theta = \frac{-2 \cdot \theta}{F_{\mathrm{f}}}, \tag{1}$$

$$\Delta x = \frac{-2 \cdot \theta \cdot H}{T}, \tag{2}$$

where F_{f} and T are the beam pointing conversion proportion and the beam position conversion proportion. Note that the negative sign in Eqs. (1) and (2) occurs because the drifts require the FSM angles are 180° out of phase with the drifts. Combination of the proportion
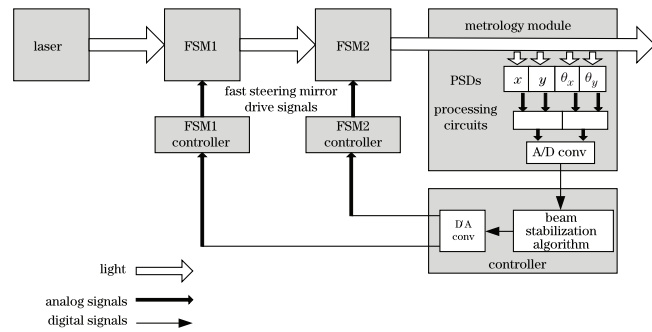

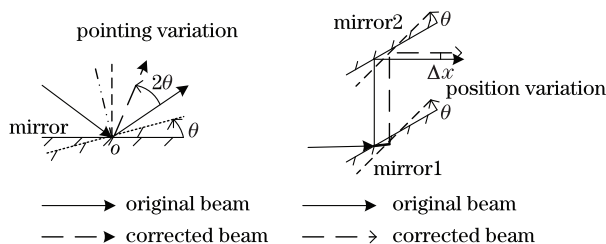Fig. 2. General structure of closed-loop system.

Fig. 3. Beam drifting correction.

relationship between BSU and BMU, we can achieve the control signal directly and quickly.

When rotating the mirror to correct beam pointing, there is an undesirable position displacement on the PSD of measuring position. Therefore, we choose FSM-2 which is closer to the output plane for achieving beam pointing correction to reduce the coupling.

Besides, Each FSM has two rotating axes to control the vertical and horizontal beam independently. In fact, there have existed coupling between two rotating axes which has an influence on the system bandwidth. This can prove that during the steering processing, coupling will be convergence as regulative time increasing.

It is hard for the beam stabilization to achieve the precise distance H in the BSU, and the relationship between the beam pointing and position and the output of PSDs in the BMU mentioned in Eqs. (1) and (2). Then the BSU and BMU can be considered into a black box so that we can just care about the input and output relationship of the box, where the input is rotating angle of FSMs ($\theta_{\mathrm{pointing}}$, $\theta_{\mathrm{position}}$) and the output is the signal of PSDs ($x_{\mathrm{pointing}}, x_{\mathrm{position}}$). A calibration procedure should be performed to get the relationship between input and output.

Calibrating the pointing path begins by sending an angle sequence command $\theta_{\mathrm{pointing}}$ to steer the FSM-2. The result x_{pointing} presented in the pointing detector PSD will be recorded so that we can recognize the pointing linear relationship between rotating angle of FSM-2 and the result in pointing detector. Thus, the slope F of the linear relationship can be achieved by

$$F = \frac{\mathrm{d}x_{\mathrm{pointing}}}{\mathrm{d}\theta_{\mathrm{pointing}}}. \tag{3}$$

Before calibrating position path, zeroing the two FSMs is necessary. Now applying the same angle sequence command $\theta_{\mathrm{position}}$ steers the FSM-1 and FSM-2 simultaneously. Similarly, the result x_{position} presented in the position detector PSD will also be recorded. A linear relationship similar to the pointing linear relationship can be obtained, and the slope Γ is given by

$$\Gamma = \frac{\mathrm{d}x_{\mathrm{position}}}{\mathrm{d}\theta_{\mathrm{position}}}. \tag{4}$$

The calibration process can incorporate filtering, for example changing the angle sequence multiple times and averaging the results. So far the stabilization can be carried out.

For the current application, the white noise is the dominant noise source in BMU, which has a main influence on the beam stabilization performance due to the pointing and position measurements deviation. It is taken into consideration that the simple algorithm is needed in the self-developed control module during the stabilization process. The average filter is adopted to reduce the influence of the white noise on the data acquisition of the beam pointing or position samples.

The expression or the model of average filtering is often analyzed to demonstrate how to decide the indexes, such as sampling times and sampling period. The aver-

age filtering can have an expression description

$$y(k) = \frac{1}{N}\left[x(k) + x(k-1) + \cdots + x(k-(N-1))\right]$$

$$= \frac{1}{N}\sum_{i=0}^{N-1} x(k-i), \tag{5}$$

where $y(k)$ and $x(k)$ are output and input samples for the filter, and N is the sampling times. After Z transform of Eq. (5), the frequency expression of the filter can be giuen by

$$H(\mathrm{j}w) = \frac{Y(\mathrm{j}w)}{X(\mathrm{j}w)} = \frac{1}{N}\frac{\sin(\frac{N}{2}wT)}{\sin(\frac{1}{2}wT)}e^{-\mathrm{j}\frac{N-1}{2}wT}. \tag{6}$$

Then, the frequency response $A(w)$ and the phase frequency response $\varphi(\omega)$ related to N and T can be achieved from Eq. (6)

$$A(w) = \frac{1}{N}\frac{\sin(\frac{N}{2}wT)}{\sin(\frac{1}{2}wT)}, \tag{7}$$

$$\varphi(w) = -\frac{N-1}{2}wT. \tag{8}$$

It is obvious that the phase variation is linear with regard to the sampling times N and the sampling period T. Thus, there is no delay among the different frequency signals. Figure 4 demonstrates the frequency response $A(\omega)$ for the different frequencies.

Comparison of Figs. 4(a) and (b) indicates that the low-pass bandwidth will decrease with increasing the sampling times N. We adopt $N=30$ and $T=0.001$ s for the stabilization system to restrain the white noise.

Here, we can apply the way mentioned in Eqs. (1) and (2) to calculate rotating angle for the actuator of FSMs. The detail feedback control procedure can be referred to Fig. 5. Here $\Delta\theta_1$, $\Delta\theta_2$ are computed to produce the rotating angle of FSM-1 and FSM-2 every time, x_{position} is the beam real-time position, x_{pointing} is the beam real-time pointing, $x_{\mathrm{reference1,2}}$ are the position and pointing required. According to the program of beam stabilization in Fig. 5, a stable beam can be achieved. It can be seen that the correct algorithm and the filter method are simple and easy to implement. Combination of all the procedures above and even PID algorithm for FSMs[20], the whole stabilization process including filtering and calculating rotating angle is easy and simple.

Whereas the beam path and mechanical vibrations of optical devices can be reduced further by changes in the applied setup, the noise in the light source cannot and so determines the most magnitude of the deviation.
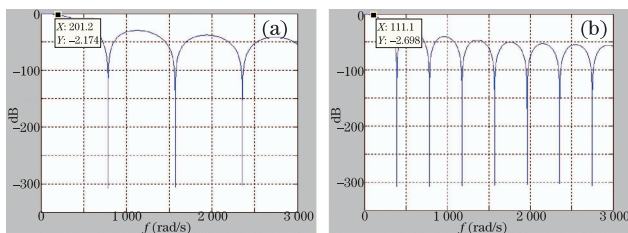

Fig. 4. Frequency response $A(\omega)$ (a) when $N=8$ and $T=0.001$ s and (b) when $N=16$ and $T=0.001$ s.
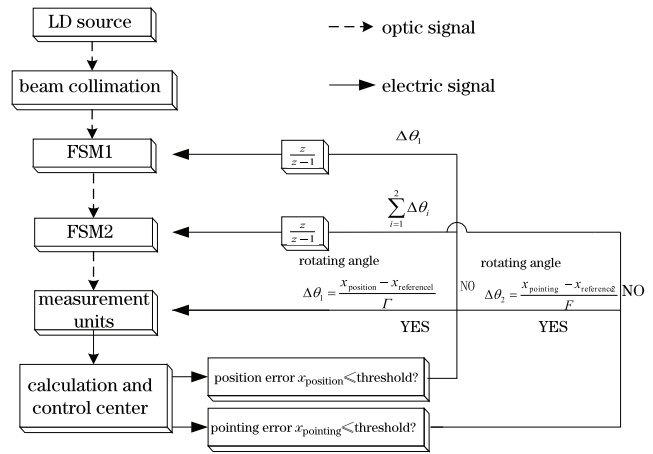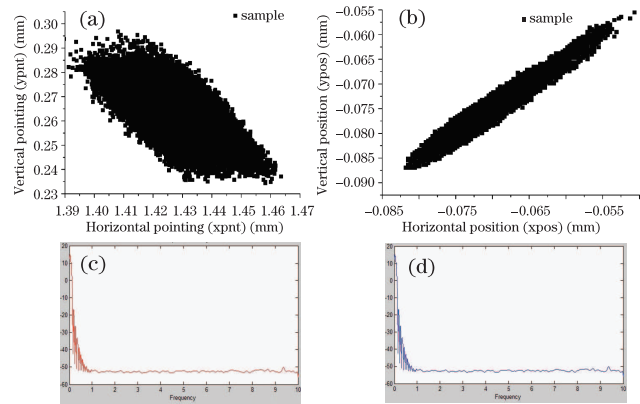

Fig. 5. Process of beam stabilization.

Fig. 6. (a) Measured beam pointing called xpnt and ypnt respectively, (b) measured beam position called xpos and ypos respectively. Both are samples from the PSDs respectively. (c) The power spectrum of beam pointing, (d) the power spectrum of beam position.

Table 1. Index of the Light Source

	Mean	Standard Deviation
Horizontal Pointing	1.42687 mrad	11.12 μrad
Vertical Pointing	0.26448 mrad	9.64 μrad
Horizontal Position	-0.55952 mm	3.296 μm
Vertical position	-0.598 mm	3.424 μm

Figure 6 shows that the beam pointing and position wander in the horizontal and vertical direction over a 20 min period and the frequency spectrum of those drifts by the Welch average method without the external interference.

The spectrum shows that the beam drift appears to be a low frequency noise with major frequency components lower than 1 Hz. This indicates that the typical movement the feedback system must respond to is the slow drift of the light source. The standard deviations of the beam pointing and position are presented in Table 1.

Hence, the stabilization method and process mentioned can be applied to the beam stabilization system to reduce the standard deviation and correct the beam pointing or position.

We have achieved the beam stability of about 8.43 μrad for the xpnt and 7.59 μrad for ypnt, and 2.16 μm for the

xpos and 2.11 μm for the ypos (both 1σ) when the close-loop control system only compensates for the light source drifting, which shows that it is possible to use the feedback system to reduce the angular and position standard deviations. To understand the performance by using the method furthermore, it is necessary to plot the target figure which is given by Fig. 7.

First of all, the beam pointing and position are corrected to the center of the target from the closed to center or the fringe of target, which is the fundamental function for the stabilization system. It can be seen that the beam pointing and position almost all are located in the red circle for the threshold the stabilization processes set up except for initial deviation. This indicates that the modified system can satisfy the beam stabilization requirements, such as accuracy and repetition.

Figure 8 shows the regulating times of correcting the single error from the system mentioned in Ref. [19] to the current system, where the two systems only have a difference about the stabilization method. The regulating time can be shortened from 110 to 84 ms. Compared with the results of the stabilization system in Ref. [19] using the matrix algorithm achieving, the angular standard deviation can be reduced to 4.2 μrad, and the position standard deviation can still keep the remained station.

However, it is not enough to only correct the beam error due to the light source drifting. One can insert a plane or a wedge, and rotate the plane to simulate the beam position drifts, and rotate the wedge to simulate the beam pointing drifts during the beam stabilization. Figure 9 shows the results the system can achieve for implementing the extra disturbances.

Figures 9(a) and (b) illustrate the beam pointing stabilization results from the PSDs directly where the obvious glitches denote the introduction of the external interference. Figures 9(c) and (d) illustrate the beam position
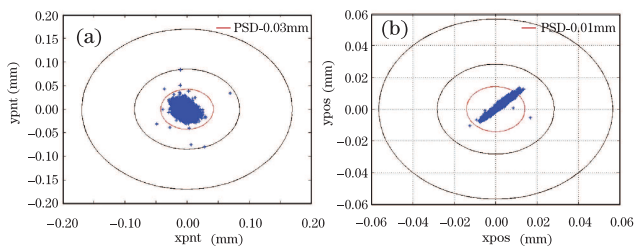

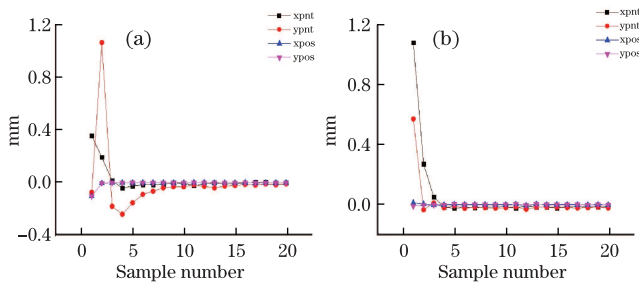Fig. 7. (a) The beam pointing targeting; (b) the beam position targeting.

Fig. 8. (a) Sensor result by using the matrix algorithm, and sampling period $T=11$ ms; (b) sensor result by using the current stabilization method, and sampling period $T=28$ ms.
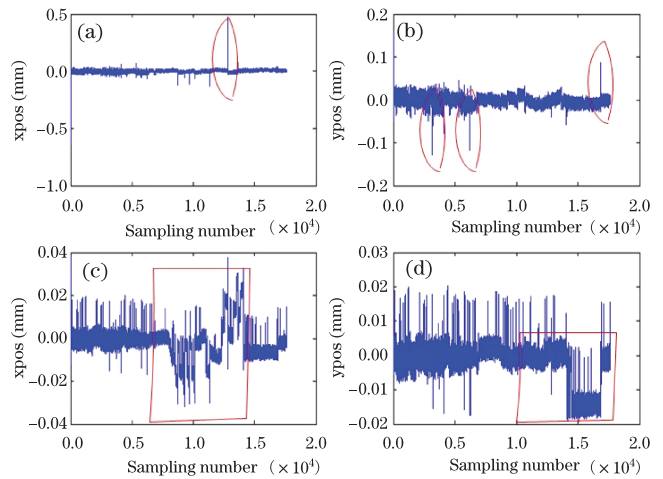

Fig. 9. Stabilization results from the PSDs with the extra disturbances.

stabilization results from the PSDs where the red rectangular denotes the introduction of the external interference. For the pointing errors, the system can correct them quickly, while the delay appearing for the position errors correction is concerned on the continuous introduction of the position errors. In a word, the stabilization system can also correct the beam drifts which come from external disturbance of position and pointing.

In conclusion, the current beam stabilization system for implementing the simple method can provide a better performance than that of utilizing the matrix algorithm obtaining under using the same hardware system. The results shows that the system using the current method can satisfy the requirements in lithography tools, such as the pointing error less than 50 μrad, the position error less than 0.5 mm, and regulating time less than 200 ms. Besides, the control program can also be simplified greatly with the simple way. Thus the method presented in this letter is effective for the current stabilization system applied in lithography tools and the key components that include BSU and BMU can be installed into lithography tools directly.

References

1. D. X. Hammer, R. D. Ferguson, C. E. Bigelow, N. V. Iftimia, T. E. Ustun, G. D. Noojin, D. J. Stolarski, H. M. Hodnett, M. L. Imholte, S. S. Kumru, M. N. McCall, C. A. Toth, and B. A. Rockwell, Proc. SPIE **6138,** 613811 (2006).
2. S. K. Dixit, R. Mahakud, O. Prakash, R. Biswal, and J. K. Mittal, Opt. Commun. **281,** 2590 (2008).
3. R. Mahakud, O. Prakash, S. K. Dixit, and J. K. Mittal, Opt. Commun. **282,** 2204 (2009).
4. A. Abramovici, W. E. Althouse, R. W. P. Drever, Y.Gürsel, S. Kawamura, F. J. Raab, D. Schoemaker, L. Sievers, R. E. Spero, K. S. Thorne, R. R. Vogt, R. Weiss, S. E. Whitcomb, and M. E. Zucker, Science **256,** 325 (1992).

5. P. W. McKenty, T. C. Sangster, M. Alexander, R. Betti, R. S. Craxton, J. A. Delettrez, L. Elasky, R. Epstein, A. Frank, V. Y. Glebov, V. N. Goncharov, D. R. Harding, S. Jin, J. P. Knauer, R. L. Keck, S. J. Loucks, L. D. Lund, R. L. McCrory, F. J. Marshall, D. D. Meyerhofer, S. P. Regan, P. B. Radha, S. Roberts, W. Seka, S. Skupsky, V. A. Smalyuk, J. M. Soures, K. A. Thorp, M. Wozniak, J. A. Frenje, C. K. Li, R. D. Petrasso, F. H. Seguin, K. A. Fletcher, S. Padalino, C. Freeman, N. Izumi, J. A. Koch, R. A. Lerche, M. J. Moran, T. W. Phillips, G. J. Schmid, and C. Sorce, Phys. Plasmas **11**, 2790 (2004).

6. E. Brambrink, H. G. Wei, B. Barbrel, P. Audebert, A. Benuzzi-Mounaix, T. Boehly, T. Endo, C. Gregory, T. Kimura, R. Kodama, N. Ozaki, H. S. Park, M. R. le Gloahec, and M. Koeing, Phys. Plasmas **16**, 033101 (2009).

7. H. Wang, F. Chen, S. Shou, and X. Song, J. Appl. Opt. **31**, 909 (2010).

8. G. C. Carl, K. H. Ralf, T. K. Paul, G. S. Pati, and M. L. Schattenburg, in *Proceedings of the 16th Annual Meeting of the American Society of Precision Engineering* 10 (2001).

9. G. C. Carl, K. H. Ralf, T. K. Paul, G. S. Pati, and M. L. Schattenburg, J. Vac. Sci. Technol. **20**, 3071 (2002).

10. F. Liu, J. Zhu, J. Xu, Q. Shan, K. Xiao, and X. Zhang, Chin. Opt. Lett. **10**, 041402 (2012).

11. H. Yan and J. Wei, Photon. Res. **2**, 020051 (2014).

12. R. Tao, X. Wang, H. Xiao, P. Zhou, and L. Si, Photon. Res. **1**, 040186 (2013).

13. T. Kanai, A. Suda, S. Bohman, M. Kaku, S. Yamaguchi, and K. Midorikawa, Appl. Phys. Lett. **92**, 061106 (2008).

14. F. Breitling, R. S. Weigel, M. C. Downer, and T. Tajima, Rev. Sci. Instrum. **72**, 1339 (2001).

15. R. A. Hardin, Y. Liu, C. Long, A. Aleksandrov, and W. Blokland, Opt. Express **19**, 2874 (2011).

16. J. Bao, L. Huang, A. Zeng, B. Ren, B. Yang, X. Peng, X. Hu, and H. Huang, Chin. J. lasers **39**, 0908004 (2012).

17. Y. Wu, D. French, and I. Jovanovic, Opt. Lett. **35**, 250 (2010).

18. P. Fritschel, N. Mavalvala, D. Shoemaker, D. Sigg, M. Zucker, and G. Gonzalez, Appl. Opt. **37**, 6734 (1998).

19. J. Wang, L. Huang, L. Hou, G. He, B. Ren, A. Zeng, and H. Huang, Proc. SPIE **9046**, 90460S (2013).

20. Z. Zheng, C. Li, B. Li, and S. Zhang, Chin. Opt. Lett. **11**, 110101 (2013).